

5-2015

POST-TRANSLATIONAL REGULATION OF ZEB1 CONTRIBUTES TO TGF β -MEDIATED EMT

Roxsan Manshour

Follow this and additional works at: http://digitalcommons.library.tmc.edu/utgsbs_dissertations

 Part of the [Medicine and Health Sciences Commons](#)

Recommended Citation

Manshour, Roxsan, "POST-TRANSLATIONAL REGULATION OF ZEB1 CONTRIBUTES TO TGF β -MEDIATED EMT" (2015). *UT GSBS Dissertations and Theses (Open Access)*. Paper 591.

This Thesis (MS) is brought to you for free and open access by the Graduate School of Biomedical Sciences at DigitalCommons@The Texas Medical Center. It has been accepted for inclusion in UT GSBS Dissertations and Theses (Open Access) by an authorized administrator of DigitalCommons@The Texas Medical Center. For more information, please contact laurel.sanders@library.tmc.edu.

POST-TRANSLATIONAL REGULATION OF ZEB1 CONTRIBUTES TO TGFB-MEDIATED EMT

by
Roxsan Manshoury

APPROVED:

Advisory Professor
Don L. Gibbons, M.D., Ph.D.

Lauren A. Byers M.D.

Faye M. Johnson, M.D., Ph.D.

Jonathan M. Kurie, M.D.

Hesham M. Amin M.D.

APPROVED:

Dean, The University of Texas
Graduate School of Biomedical Science at Houston

POST-TRANSLATIONAL REGULATION OF ZEB1 CONTRIBUTES TO TGFB-MEDIATED EMT

A

MASTER'S THESIS

Presented to the Faculty of
The University of Texas
Health Science Center at Houston

and

The University of Texas
MD Anderson Cancer Center
Graduate School of Biomedical Sciences
in Partial Fulfillment
of the Requirements
for the Degree of

MASTER'S OF BIOMEDICAL SCIENCE

by

Roxsan Manshoury, B.S., M.S.
Houston, Texas
May 2015

Acknowledgements

I would like to thank my thesis advisor, Dr. Don Gibbons, who has been a wonderful mentor throughout these past two years. He has continuously challenged, encouraged, and amused me. Thank you for taking the chance on me. I look forward to continuing my studies with you in the fall for the beginning of my Ph.D candidacy.

Thank you to all my committee members Drs. Hesham Amin, Faye Johnson, Lauren Byers, Jonathan Kurie for their constructive feedback and support. I would especially like to acknowledge Dr. Amin, who has been instrumental to my education here at MD Anderson. His mentorship throughout my formative years was extremely influential to my decision to pursue my studies at GSBS and I will always be grateful.

I'd like to thank the members of the Gibbons' lab for their support. I would specifically like to thank Dr. Samrut Kundu who patiently trained me and has continued to help me develop this project. I would also like to thank Drs. Christin Ungewiss and Jonathon Roybal for answering every foolish question — admittedly there were quite a few. Both have guided me scientifically and have made every day at work too much fun.

Aside from work, I would like to acknowledge my parents and Alex for all their encouragement. Thank you to my father who has inspired my decision to pursue a career in this field and who has been an attentive study partner when needed. And thank you Alex, who has stabilized me throughout the stressful moments and has provided the laughter to revitalize me after draining work days. Thank you for being there for me.

Post-translational regulation of ZEB1 contributes to TGF β -mediated EMT

Roxsan Manshouri

Mentor: Don L. Gibbons, MD, PhD

Non-small cell lung cancer (NSCLC) is the leading cause of cancer-related death in the United States due in part to the affinity of tumors to metastasize. Understanding the process which contributes to metastasis provides promise for the discovery of novel therapeutic targets. Epithelial-to-mesenchymal transition (EMT) is a proposed model for the initiation of metastasis. During EMT epithelial cells lose their cell adhesion properties and acquire a mesenchymal-like phenotype, allowing tumor cells to migrate from their epithelial cell community and invade remote locations. EMT is mediated by several signaling pathways, with transforming growth factor-beta (TGF- β) receiving attention for its up-regulation in the metastatic tumor microenvironment. TGF- β facilitates EMT through a variety of mechanisms but a prominent feature of TGF- β induced EMT is the activation of the transcription factor zinc finger E-box-binding homeobox 1 (Zeb1). Although Zeb1 has an established role in EMT the mechanism by which Zeb1 is regulated has not been fully elucidated. Here we demonstrate that Zeb1 undergoes post-translational modification and that this modification contributes to protein stability. We also expose novel Zeb1 interactions using the BioID method for proximity-dependent labeling of proteins. These results lead us to hypothesize that by targeting factors that mediate Zeb1 post-translational modification we may provide a therapeutic approach for metastasis suppression in NSCLC.

Table of Contents

Approvals	i
Titles	ii
Acknowledgements	iii
Thesis Abstract	iv
Table of Contents	v
List of Illustrations	vii
List of Tables	viii
Abbreviations	ix
Chapter 1: Introduction	1
Lung Cancer	2
Epithelial-to-mesenchymal transition	3
Zinc finger E-box binding homeobox 1	4
Chapter 2: Materials and Methods	5
Cell Culture	8
RNA interference	8
Quantitative RT-PCR Analysis	9
Lambda Phosphatase incubation	9
Immunoblot	10
Immunoprecipitation (IP)	10
Cycloheximide treatment	11
3D culture	11
Migration and Invasion Assay	11

BioID system	12
Chapter 3: Results	14
Comparison of TGF- β and Zeb1 induced EMT	15
Knockdown reveals the significance of ZEB1 expression during EMT	20
Immunoprecipitation of GFP-tagged ZEB1	23
Post-translational modification prolongs the half-life of ZEB1 protein	28
BioID method can expose the ZEB1 interactome	31
Chapter 4: Discussion	36
Bibliography	41
Vita	45

List of Illustrations

Fig. 1 Zinc finger E-box binding homeobox 1 (ZEB1) protein structure.....	5
Fig. 2 344SQ cells undergo EMT upon addition of TGF- β	15
Fig. 3 Characterization of 393P cells with inducible Zeb1 expression.....	16
Fig. 4 344SQ-GFP-Zeb1 cells undergo an EMT similar to TGF- β treatment.....	17
Fig. 5 3D culture of 344SQ-GFP-Zeb1 cells	19
Fig. 6 Zeb1 knock down in invasive 344SQ cells.....	21
Fig. 7 Knock down of Zeb1 in invasive cells does not affect response to TGF- β	22
Fig. 8 3D-culture of Zeb1 knockdowns confirms Zeb1 is not required for TGF- β mediated EMT.	24
Fig. 9 Immunoprecipitation of GFP fused Zeb1.....	25
Fig. 10 Lambda phosphatase treatment of NSCLC cell lines confirms ZEB1 phosphorylation.....	27
Fig. 11 Immunoprecipitation of the endogenous ZEB1.....	29
Fig. 12. Translational inhibition show differential effect between ZEB1 species.....	27
Fig. 13 C-terminal tagged Zeb1-Flag-BirA* is biologically active.....	32
Fig. 14 N-terminal tagged Zeb1-Flag-BirA* is biologically active.....	33
Fig. 15 Schematic depicting potential interactions captured by BioID system.....	35

List of Tables

Table 1. Primer sequences used for qRT-PCR analysis.....	9
Table 2. List of antibodies used for Western Blot analysis.....	10
Table 3. List of ZEB1-BirA cloning primer.....	12

Abbreviations

3'-UTR	three prime untranslated region
bp	base pairs
CDH1	Cadherin 1, E-Cadherin
CDH2	Cadherin 2, N-Cadherin
Coll	Collagen Type I
Dox	Doxycycline
EMT	epithelial-to-mesenchymal transition
GFP	green fluorescent protein
IgG	Immunoglobulin G
KD	knockdown
kDa	kilodalton
Lambda PP	Lambda Phosphatase
LN	lymph node
MET	mesenchymal-to-epithelial transition
MG	Matrigel
miR	microRNA
mRNA	messenger ribonucleic acid
NSCLC	non-small cell lung cancer
PBS	Phosphate buffered saline
qRT-PCR	quantitative real-time polymerase chain reaction
RIPA buffer	radioimmunoprecipitation assay buffer
RT-PCR	Real Time Polymerase Chain Reaction
scr	scramble control
shRNA	short hairpin RNA

SQ	subcutaneous
TBST	Tris-buffered Saline and Tween 20
TGF- β	transforming growth factor beta
Vim	Vimentin
wt	wild type
ZEB1	Zinc finger E-box binding homeobox 1

Chapter 1:

Introduction

Lung cancer

Lung cancer is the current leading cause of all cancer related death in the United States [1]. There are two major types of lung cancer: non-small cell lung cancer (NSCLC) and small cell lung cancer (SCLC). NSCLC constitutes approximately 85% of lung cancers and comprises of three subtypes: squamous cell carcinoma, large cell carcinoma, and adenocarcinoma--the most common histologic type [2]. Poor patient prognosis is primarily due to the affinity of tumors to develop metastasis leading to advanced disease at the time of diagnosis. Nearly two-thirds of lung cancer patients are diagnosed with late stage disease and of patients who undergo surgery approximately half will develop recurrence with metastatic disease [2]. Despite ongoing research, much of which has focused on understanding tumor emergence and eradication, the mortality rate of lung cancer patients has changed very little, due in part to the incomplete understanding of the metastatic process.

With the intention of studying the biologic processes driving lung cancer progression and metastasis, several genetic mouse models have been generated which are capable of developing lung adenocarcinoma. In particular, the $Kras^{LA1}p53^{R172HDG}$ (KP) genetically engineered mouse model was found to recapitulate features of metastasis-prone lung cancer patients [3]. A panel of lung adenocarcinoma cell lines were derived from the KP model from various primary and metastatic tumor sites and were subcutaneously injected into syngeneic mice to confirm their propensity to metastasize [4]. The cell line 393P (derived from primary lung tumor) was defined as a metastasis incompetent cell line, 344SQ (subcutaneous metastasis) was a metastasis prone cell line, and 393LN (lymph node metastasis) was capable of intermediate metastasis. This evaluation was based on 393LN ability to produce lung

metastases when injected by tail vein or intra-cardiac injection, but not subcutaneously, while 393P cells were not able to form lung metastases through either method [3].

Using 393P as a reference control, these three cell lines were transcriptionally profiled to reveal differential gene expression between metastatic and non-metastatic tumors. The genes associated with metal ion binding and zinc ion binding were found to be up-regulated in the 344SQ tumor compared to the 393P tumor, whereas the genes categorized as tight junction, cell differentiation, and multicellular organismal development were down-regulated. Based on these characteristics it was determined that the 344SQ tumor profile was consistent with cells undergoing the biological process epithelial-mesenchymal transition (EMT) [4].

Epithelial-mesenchymal transition

EMT is the mechanism by which epithelial cells lose their apical-basal polarity and specialized cell contacts to acquire migratory behavior and mesenchymal-like phenotype [5]. EMT enables cells to detach from the epithelial cell layer from which they originate and invade remote locations where they may then undergo mesenchymal-epithelial transition (MET), the reversion to an epithelial phenotype. Several distinct molecular mechanisms are involved in EMT including reorganization of the active cytoskeleton, activation of transcription factors, increased resistance to apoptosis and production of ECM-degrading enzymes, as well as changes in microRNA expression[6]. This process is integral to wound healing and embryonic development; however, activation of EMT has also been proposed as the crucial mechanism for the initiation of metastatic dissemination by epithelial cancer cells [6].

Induction of an EMT has been associated with the expression of numerous mesenchymal markers such as vimentin and N-Cadherin. Once malignant cells have successfully

micro- and macro-metastasized these cells then undergo MET whereby they regain epithelial markers such as E-Cadherin and Crb3 to facilitate secondary tumor colonization [6]. EMT is induced by multiple signals originating from the tumor-associated stromal cells. Growth factors such as HGF, EGF, PDGF, and TGF- β mediate EMT through regulation of the transcription factors Snail, Slug, Twist, and most notably zinc finger E-box binding homeobox 1 (ZEB1). When expressed, these transcription factors orchestrate EMT through the regulation of genes associated with the epithelial phenotype [6].

Zinc finger E-box-binding homeobox 1

ZEB1 is a 124 kDa transcription factor which is characterized by two terminal flanking zinc finger clusters allowing for binding to the E-box typically located in the promoter of the target gene, as well as a centrally located homeobox domain (Fig. 1). Originally identified for its role in cell differentiation and embryogenesis, the ability of ZEB1 to induce an EMT has defined ZEB1 as an important factor in metastasis [7]. In fact, dysregulation of ZEB1 has been associated with tumor progression in NSCLC and several other cancer types [8-10], thus understanding the regulation and role of ZEB1 in EMT could provide a therapeutic approach to the control of metastatic disease.

ZEB1 facilitates EMT through the regulation of several genes responsible for an epithelial phenotype such as epithelial cell polarity genes, classical cadherins, desmosome proteins, tight and gap junction proteins, apical and vesicle transport proteins, and epithelial cell surface receptors [11]. In particular, ZEB1 direct transcriptional repression of E-Cadherin—a central component in cell-cell adherens junction—in human cancer cell has established ZEB1 as a master regulator of epithelial cell plasticity [12].

Protein domains:



PREDICTED molecular weight: 124 kDa

Fig. 1 Zinc finger E-box binding homeobox 1 (ZEB1) protein structure. ZF: Zinc finger domain; SMAD: Smad-binding domain, contributes to TGF- β target gene transcription; HD: Homeodomain; CtBP: C-terminal-binding protein 1 interaction domain, contributes to transcriptional repression; NLS: nuclear localization signal.

ZEB1 involvement in a negative feedback loop with the miR-200 family members has recently been described in various carcinomas [13]. The family consists of five members (miR-200a, miR-200b, miR-200c, miR-141, and miR-429) located in two clusters: miR-200a, miR200b, miR-429 and miR-200c, miR-141. ZEB1 directly represses the miR-200 family through direct binding to the promoter regions thus forming a regulatory loop which is responsible for maintain cells in an epithelial or mesenchymal phenotype. Conversely, ZEB1 is a target of the miR-200 family [14]. Down-regulation of the miR-200 family in metastatic NSCLC cells has been reported and has been shown to be necessary and sufficient to initiate EMT [4].

Although ZEB1 has a predicted molecular weight of 124 kDa several groups have reported discrepancies in the observed molecular weight (approximately 225 kDa) [15]. The interplay between ZEB1 and various co-repressors and co-activators regulate ZEB1 activity under specific conditions through post-translational modification (PTM) [15-18]. In human cholangiocarcinoma cell lines, HuCCT1, the histone acetyltransferases p300 and p/CAF was revealed to acetylate ZEB1, resulting in release of ZEB1 transcriptional suppression of target genes [17]. Additionally, in a radioresistant subpopulations of breast cancer cells it was found that ATM phosphorylates and stabilizes ZEB1 in response to DNA damage, thereby promoting DNA repair and radiation resistance [15]. Despite the dissimilarity between the predicted and observed ZEB1 size, no group has been able to account for the total difference in molecular weight. In particular, few have shown the role of PTMs in regulating ZEB1 function. Here we show that ZEB1 is post-translationally modified in NSCLC and that this modification is essential to TGF- β mediated EMT.

Chapter 2:

Materials and Methods

Cell Culture

Human lung cancer cell lines H1155, H157, H441 and H358 were obtained from the National Cancer Institute (NCI-H series) or the Hamon Center for Therapeutic Oncology Research, University of Texas Southwestern Medical Center (HCC series). Cell lines from the p53^{R172HAg/+} K-ras^{LA1/+} mice were derived and maintained as previously described [4]. Cell line names depict the mouse number and site of derivation (e.g., 393P was derived from primary lung tumor). HEK/293 Flp-In T-Rex were provided by the Raught laboratory (University of Toronto) and were cultured in DMEM with 0.4% Hygromycin B. All other cell lines were cultured and passaged in RPMI 1640 supplemented with 10% fetal bovine serum (FBS) and incubated in 5% CO₂ at 37°C. The pTRIPZ-GFP [19] inducible cell lines as well as H157-Tripz-miR200ab were cultured in full RPMI media with puromycin. Cells were incubated with recombinant human TGF-β1 (Cell Signaling 8915LF) at 5 ng/mL.

RNA Interference

TRC Lentiviral pLKO.1 plasmid expressing scrambled control shRNA or murine ZEB1 shRNA (RHS4080) were purchased (ThermoScientific), containing the following ZEB1-specific shRNAmir sequences: 5' - AAACCCAGGGCTGCCTTGAAAAG - 3' (shRNA-mZEB1-1: TRCN0000070819) and 5' - AAACCCAGGGCTGCCTTGAAAAG - 3' (m-shRNA-mZEB1-3: TRCN0000070822). 344SQ and 531LN2 cells were virally infected as previously described [20] and cultured in RPMI 1640 with 10% FBS and puromycin.

Quantitative Real-Time PCR Analysis

Total RNA was extracted using TRIzol® Reagent (Life Technologies) and was isolated according to the manufacturer's instructions. Analysis of mRNA levels was performed on a 7500 Fast Real-Time PCR System (Applied Biosystems) with SYBR® Green Real-Time PCR, using primers designed using the NIH primer design tool. The ribosomal housekeeping gene L32 was used as an internal control and data was analyzed with the 7500 Software v2.0.5 (Applied Biosystems). Student's *t*-test was performed for statistical significance.

qRT-PCR primer 5' to 3'

ms L32	GGAGAAGGTTCAAGGGCCAG
ms L32: R	TGCTCCATAACCGATGTTG
ms Zeb1: F	ATGCTCGAACGCGCAGC
ms Zeb1: R	AATCGGCGATCTTTGAGAGCT
ms CDH1: F	CCTCTCAAGCTCGCGGATA
ms CDH1: R	TCCAACGTGGTCACCTGGT
ms CDH2: F	TCCAFAFFATCAAAGCCTGGGAC
ms CDH2: R	CCGCATCAATGGCAGTGACCGT
ms Vim: F	TCCAAGCCTGACCTCACTGC
ms Vim: R	TTCATACTGCTGGCGCACAT
hs L32: F	CCTTGTGAAGCCCAAGATCG
hs L32: R	TGCCGGATGAACTTCTTGGT
hs Zeb1: F	GGCATAACCTACTCAACTACGG
hs Zeb1: R	TGGGCGGTGTAGAATCAGAGTC
hs CDH1: F	TTTACCCAGCCGGTCTTTGA
hs CDH1: R	TCCTGGAACAGCGCCTTCT

Lambda Phosphatase incubation

Cells were lysed with 1 x NEBuffer for PMP supplemented with 1 mM MnCl₂ or with 1 X RIPA Buffer (Cell Signaling 9806). Lysates harvested in the PMP buffer (30 µg) was treated with 400 units of lambda-phosphatase/20 µL for 30 min. at 37° C. Samples were immediately separated on an SDS polyacrylamide gel and transferred onto a nitrocellulose membrane.

Immunoblot

Protein estimation was conducted by use of the Pierce™ BCA Protein Assay Kit (Thermo Scientific, Cat. No. 23227). Samples were separated on SDS polyacrylamide gels and transferred onto a nitrocellulose membrane. The membranes were blocked using 5% nonfat dry milk and incubated in primary antibody overnight at 4°C (see Table 2 for antibody list). Membranes were exposed using ECL (GE Healthcare) per the manufacturer's instructions.

Gene	Company	Catalog No.
Zeb1	Santa Cruz	H-102
Zeb1	Cell Signaling	3396
normal mouse IgG	Santa Cruz	SC-2025
normal rabbit IgG	Santa Cruz	SC-2027
E-Cadherin	B&D	160182
Vimentin	Cell Signaling	3932
Flag	Sigma	F1804
GFP	Santa Cruz	SC-9996
B-actin	Sigma	A1978
Phospho-(Ser/Thr) Phe	Cell Signaling	9631
Phospho-Tyrosine,	Cell Signaling	9411
Acetylated Lysine	Cell Signaling	9441

Immunoprecipitation (IP)

Cell lines 393P-TG-Zeb1 and 393P-TG-Vec were cultured in 2 µg/ml doxycycline (dox) for 24 h to induce GFP-Zeb1 production prior to lysis. Pull-down assays were performed using 500 µg of crude lysate incubated overnight with 200 µg/ml anti-GFP (SC-9996) at 4° C and gentle agitation. Protein A/G PLUS-Agarose Immunoprecipitation Reagent (SC-2003) was then introduced for 2 hrs. Antibody-antigen complexes were washed with phosphate-buffered saline (PBS) and Wash Buffer (50 mM Tris (pH 7.4), 150 mM NaCl, 1 mM EDTA, 1% Triton X-100), eluted with 1 x RIPA buffer at 100° C and separated by SDS-PAGE before Western blot analysis.

Cycloheximide chase experiment

Wild type 393P and 344SQ cells were exposed to 100 µg/ml cycloheximide (C4859, Sigma-Aldrich) for up to 24 h. Samples were collected at the time points 0, 1, 2, 4, 8, and 24 h.

Western blot was then performed as described and quantification of immunoblot of ZEB1 was conducted using densitometry software, Image Processing and Analysis in Java (ImageJ, NIH).

Half-life was calculated by:

$$T_{1/2} = (\text{elapsed time} \times \log 2) / \log (\text{beginning amount} / \text{ending amount})$$

3D culture

Cells were grown in 3D culture on 1.2 mg/ml Matrigel/Collagen Type I (Rat tail, Corning, Product #354236) in eight-well glass chamber slides, as described (Sodunke TR et. al., 2007). A single-cell suspension containing 1500 cells was plated onto a layer of Matrigel/Collagen (BD Biosciences). The cells were grown in RPMI 1640 with 10% FBS and 2% Matrigel. Designated samples were incubated with 5 ng/mL TGF-β. Cell growth and morphology were followed by phase contrast microscopy on an Olympus IX 71 microscope.

Migration and Invasion Assay

Cells were resuspended in serum-free media and seeded in a 24-well Transwell or Matrigel plate (BD Biosciences, pore size 8 µm) at a concentration of 5×10^4 per well. RPMI supplemented with 10% FBS was added to the lower chamber and cells were allowed to migrate for 16 h in 5% CO₂ at 37°C. Migrating cells were stained with 0.1% crystal violet. Non-migrating cells were removed using a cotton swab. Migrated cells were quantified based on five microscopic fields at a 4X magnification and results were represented as mean ± standard

deviation and student's *t*-test was performed for statistical significance. Each assay was performed in triplicate.

BioID system

Zeb1 was cloned from the pLenti-GIII-CMV-hZEB1-GFP-2A-Puro lentiviral vector (Applied Biological Materials Inc., LV362466, Accession No. BC112392) using PCR amplified with primers containing *Asc*I and *Not*I (N-terminus tag) or *Kpn*I and *Not*I (C-terminus tag) restriction enzyme sites and cloned in to the pcDNA5 FRT/TO FLAG-BirAR118G (pcDNA5 Flag-BirA*)[21] vectors provided by Dr. Brian Raught (University of Toronto).

Primer name	Sequence 5' to 3'
Flag-BirA-[ZEB1] <i>Asc</i> I -F	tataGGCGCGCCaATGgcggatggccccaggtg
Flag-BirA-[ZEB1] <i>Not</i> I-R	ttaaGCGGCCGCaTCAggcttcattgtctttt
[ZEB1]BirA-Flag <i>Kpn</i> I -F	tataGGTACCgccaccATGgcggatggccccaggtg
[ZEB1]BirA-Flag <i>Not</i> I-R	ttaaGCGGCCGcggtggcttcattgtctttt

The N-terminus or C-terminus Flag-BirA tag vector control and Zeb1 were transfected into HEK/293 Flp-In along with pOG44 Flp-Recombinase expression vector using Lipofectamine® LTX Reagent with PLUS™ Reagent as per the manufacturer's instructions (Invitrogen, Cat. No. 15338100). Cell lines were cultured until colonies were ~3 mm in diameter at which point each was trypsinized and divided into two pools. These were considered as a biological replicate and were processed independently.

Subsequently, all cell lines were cultured in four different conditions and harvested:

- (1) DMEM + 10% FBS.
- (2) DMEM + 10% FBS + 5 μ M MG-132
- (3) DMEM + 10% FBS + 1 μ g/ml Tetracyclin and 50 μ M biotin
- (4) DMEM + 10% FBS + 1 μ g/ml Tetracyclin, 50 μ M biotin, and 5 μ M MG-132

Samples were snap-frozen and shipped on dry ice to the Raught laboratory for processing, mass spectrometry, and analysis.

Chapter 3:

Results

Comparison of TGF- β and ZEB1 induced EMT

Our group has previously shown that the tumor microenvironment of metastasis prone tumors (344SQ) have higher expression of TGF- β compared to metastasis incompetent tumors (393P) [1]. In fact, 393P tumors require a greater time of TGF- β exposure to produce a morphologic response (approximately 5-7 days) compared to 344SQ cells, which undergo an EMT within 24 h, displaying a fibroblastic-like phenotype (Fig. 2A). When both cell lines are cultured in a 3D assay in which a single cell suspension is plated on a thin Matrigel (MG) layer 393P cells grow as disorganized masses while 344SQ cells are capable of forming hollow, non-invasive epithelial spheres [4]. Upon TGF- β treatment these rounded structures are disrupted, forming invasive protrusions and becoming highly proliferative (Fig. 2B).

Our work has also demonstrated constitutive Zeb1 expression to be sufficient in inducing an invasive phenotype in 393P [22]. To fully characterize this phenotype and compare the contribution of Zeb1 during TGF- β -mediated EMT, the cell lines 393P-TripZ-GFP-Zeb1 (393P-GFP-Zeb1) and 344SQ-TripZ-GFP-Zeb1 (344SQ-GFP-Zeb1) were created, which have inducible expression of a GFP-tagged ZEB1. In both cell lines a striking phenotypic EMT was observed within 24 h of Zeb1 expression in 2D culture (Fig. 3A and 4A). EMT was also observed at the protein and mRNA level (Fig. 3B, 4B and 4C). This phenotype was similar to 344SQ cells treated with TGF- β (Fig. 2A). Correspondingly, when 344SQ cell lines were cultured in a modified 3D assay, in which a Matrigel/collagen-type I (MG/Coll) mix is used to better mimic the tumor microenvironment, the Zeb1 inducible cells which were dox induced upon plating were highly invasive and produced spindle-like protrusions (Fig. 5B). However, when 344SQ-GFP-Zeb1 cells were allowed to form spheres (7 days) prior to dox induction, spheres remained phenotypically

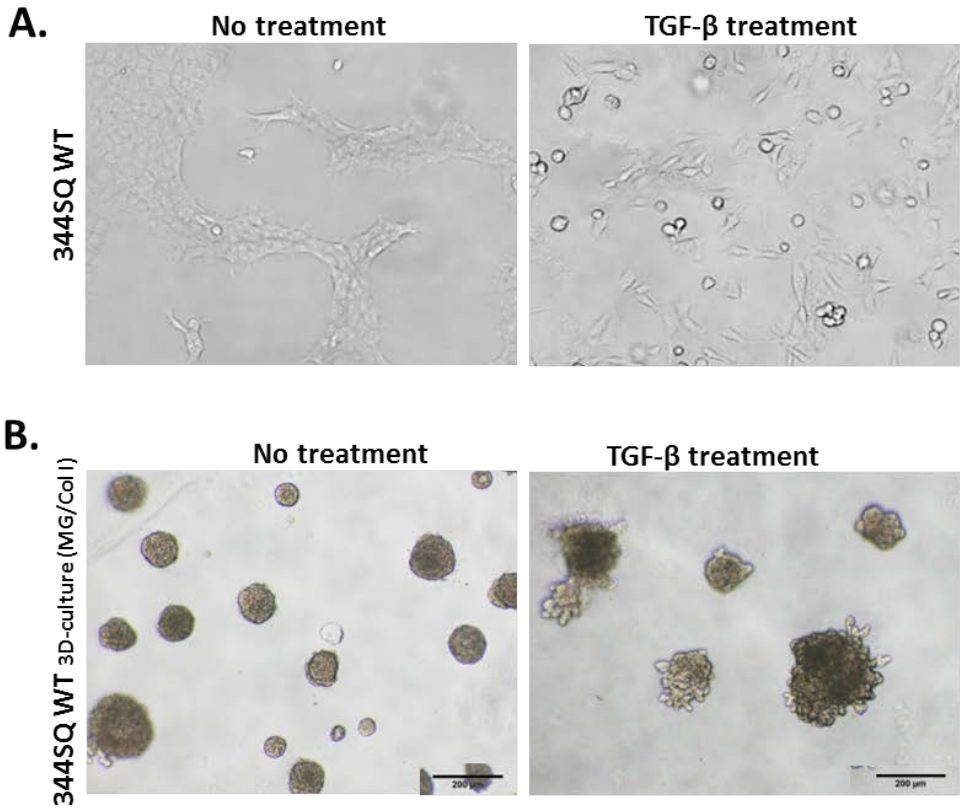


Fig. 2 344SQ cells undergo EMT upon addition of TGF- β . (A) Wild type 344SQ cells cultured with or without 5 ng/ml TGF- β for 96 h. Treated cells display a fibroblastic-like phenotype associated with EMT. (B) 3D- Matrigel/Collagen type I (1.2 mg/ml) of 344SQ cells cultured with or with out 5 ng/ml TGF- β . Treated structures are disrupted, forming invasive protrusions and becoming highly proliferative.

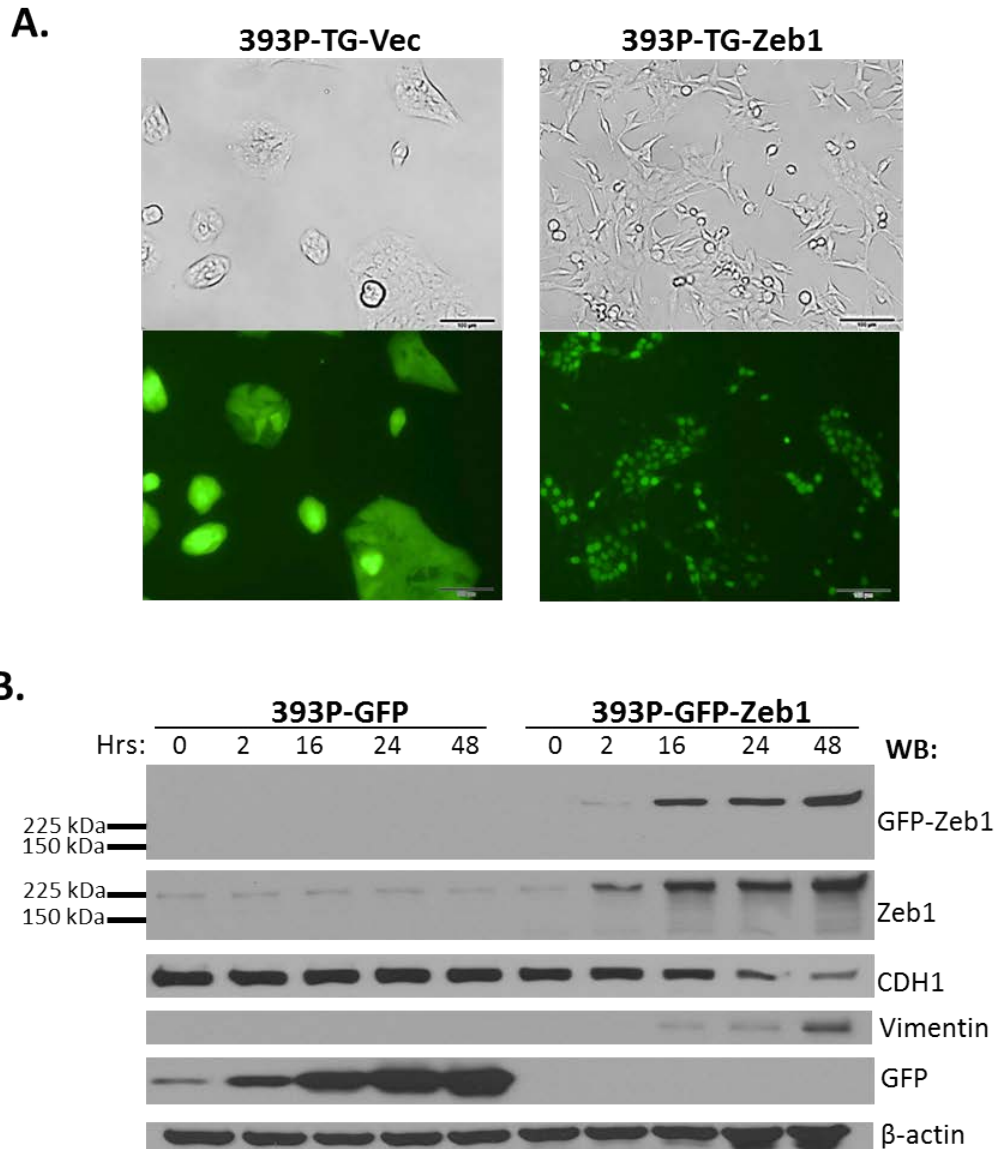


Fig. 3 Characterization of 393P cells with inducible Zeb1 expression. (A) Morphology of 393P-GFP-Zeb1 cells induced with dox for 48 hrs. Expression of GFP-Zeb1 fusion protein illustrates ZEB1 is located exclusively in the nuclear. (B) Western blots of 393P-GFPc and 393-GFP-Zeb1 time course over 48 hrs of induction. GFP fused Zeb1 appears ~24 kDa larger than endogenous Zeb1. Other EMT markers such as CDH1 and Vim were subsequently affected by Zeb1 expression, confirming an EMT.

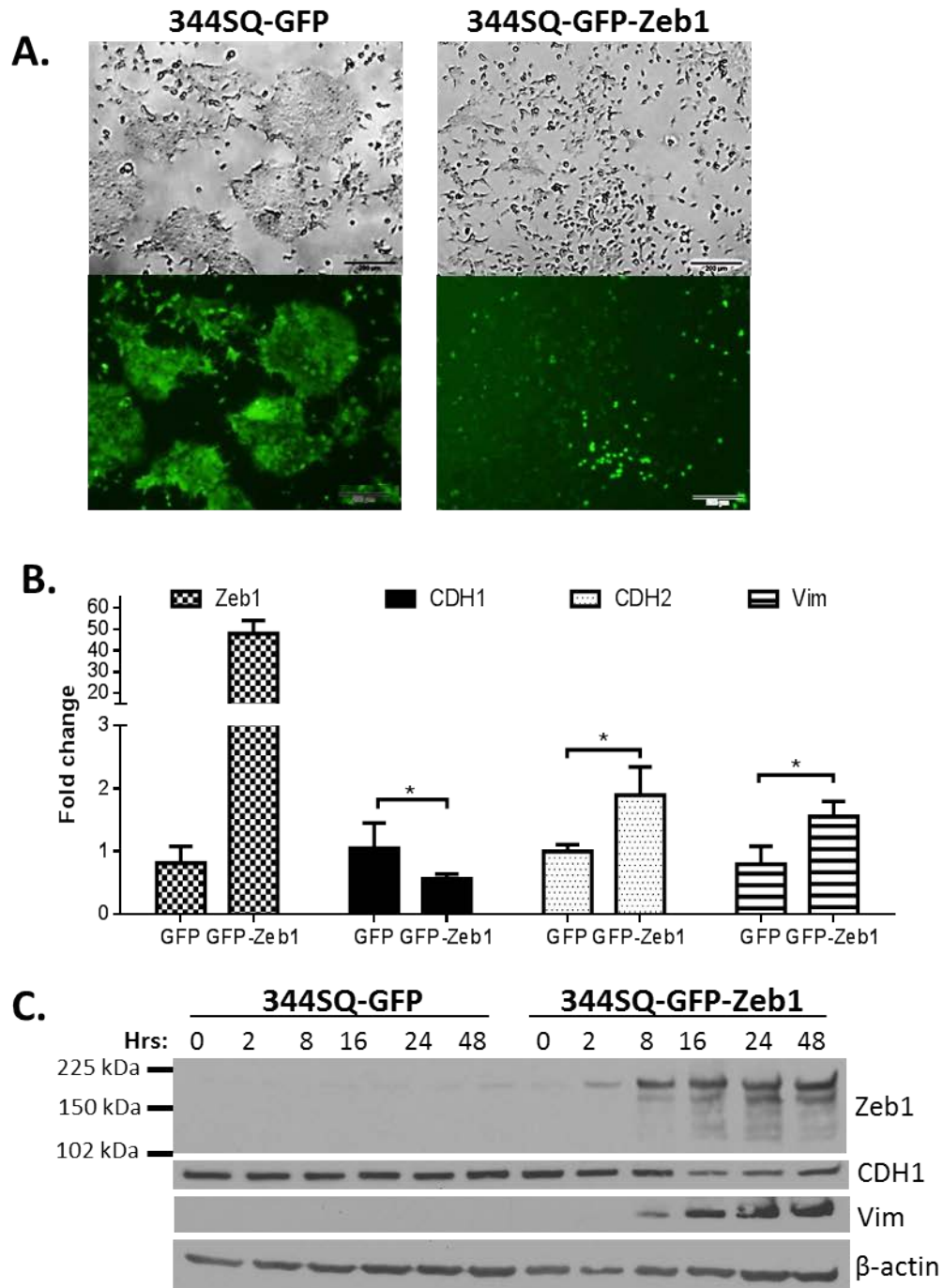


Fig.4 344SQ-GFP-Zeb1 cells undergo an EMT similar to TGF- β treatment. (A) Morphology of 344SQ cells induced with dox for 48 hrs. Induced 344SQ-GFP-Zeb1 cells resemble cells treated with TGF- β . (B) RT-qPCR of EMT markers in 344SQ-GFP-Zeb1 (GFP-Zeb1) cells induced for 48 as compared to vector control (GFP). (C) Western blot of dox induced time course of both 344SQ-GFP and 344SQ-GFP-Zeb1 verify cells are undergoing EMT.

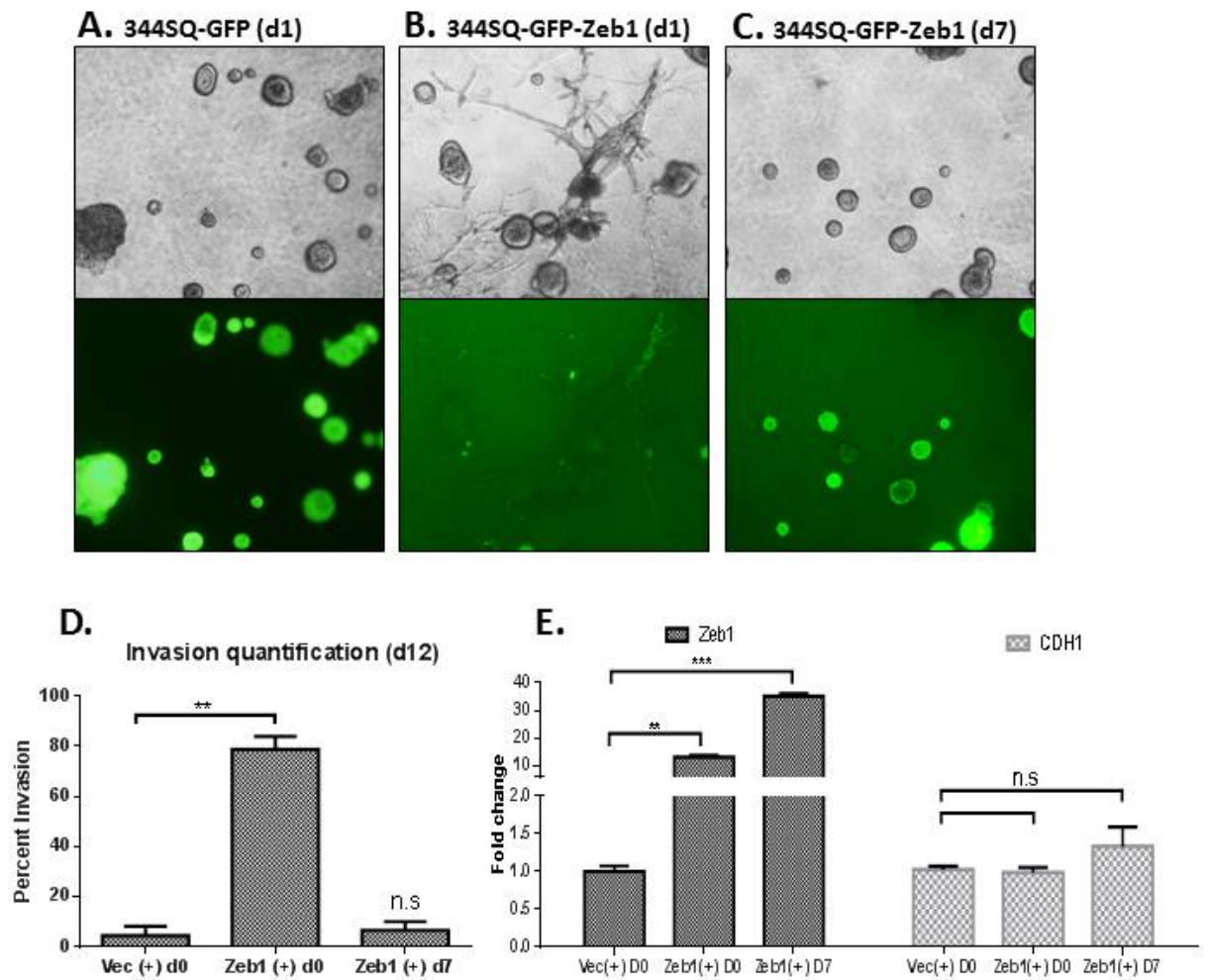


Fig.5 3D culture of 344SQ-GFP-Zeb1 cells (A) Morphology by contrast microscopy of 344SQ-GFP cells cultured and dox induced for 12 days in 3D MG/Coll assay. (B) 344SQ-GFP-ZEB1 cells supplemented with dox in growth medium on day 1 of culture (C) or on day 7. (D) Percent invasion quantified at endpoint (d12) prior to harvesting spheres for RNA isolation. (E) RT-qPCR demonstrates Zeb1 induction and response of markers Zeb1 and CDH1 during 12d 3D culture.

non-invasive (Fig. 5C). Quantification of invasion reinforce the observed phenotype (Fig. 5D) as well changes in the mRNA expression of ZEB1 and E-Cadherin (Fig. 5E). This suggests that Zeb1 is required for the invasive phenotype, but Zeb1 expression is not sufficient to overcome an epithelial state.

Knockdown reveals the significance of Zeb1 expression during EMT

To determine the significance of ZEB1 in the initiation of EMT, shRNA-Zeb1 knockdowns (KD) were generated using the 344SQ WT cells. KD was confirmed by qPCR, with 63.84% reduction seen in 344SQ-shRNA-Zeb1#1 and 47.64% reduction in 344SQ-shRNA-Zeb1#3 (Fig. 6B). This prominent effect on Zeb1 mRNA did not translate to the overall protein expression. The higher molecular weight ZEB1 (225 kDa-ZEB1) expression was affected approximately 20% in either KD compared to the lowest molecular weight ZEB1 (125 kDa-ZEB1) which was reduced nearly 70% (Fig. 6C). Despite these discrepancies Zeb1 KD produced a shift to a more epithelial phenotype, as displayed by the decrease of invasive cell protrusions (Fig. 6A).

Next we sought to assess the response of the Zeb1 KD cells to TGF- β , to examine the requirement for Zeb1 as a mediator of the TGF- β effect. In 2D assays, Zeb1 KD cells were treated with TGF- β for 96 h. EMT was observed in both KDs as compared to the phenotype (Fig. 7D) and EMT profile of the scramble (scr) by protein and mRNA (Fig. 7A, 7B and 7C) as well as by functional assays. Migration and invasion of KD cell lines were significantly increased by the addition of TGF- β to growth media (Fig. 8A and 8B). Dissimilarities were observed between the two species of ZEB1. Although ZEB1 expression did not significantly change in the scr cell line under TGF- β incubation, the 125 kDa-ZEB1 increased in both KD cell lines, while the 225 kDa-

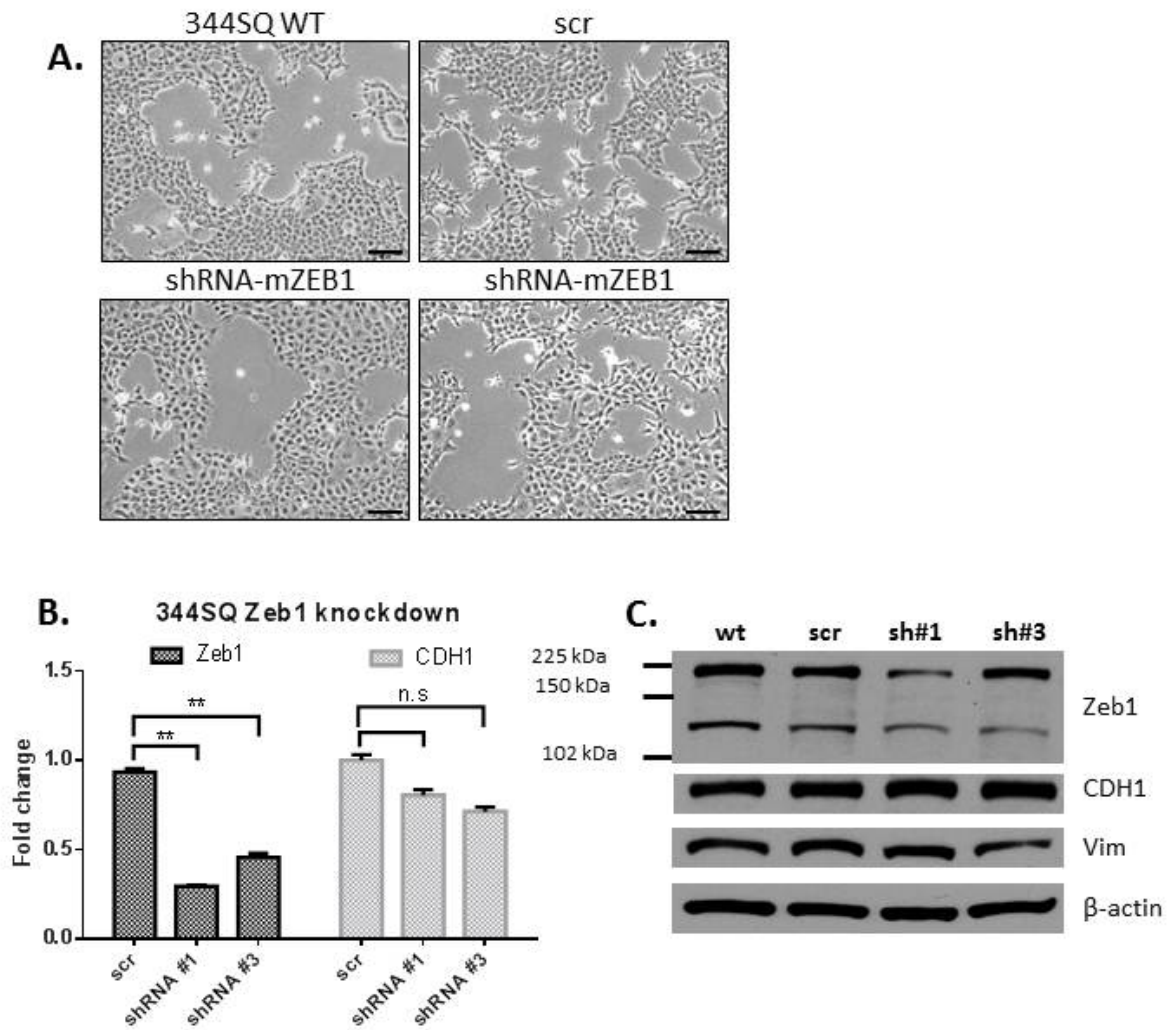


Fig.6 Zeb1 knock down in invasive 344SQ cells. (A) Morphology of 344SQ Zeb1-shRNAs. (B) Syber Green-based qRT-PCR confirms Zeb1 knockdown as compared to scramble. Samples were treated with 5 ng/ml TGF- β for 96h as indicated. (C) Western blot analysis of 344SQ Zeb1 knockdowns treated as described above.

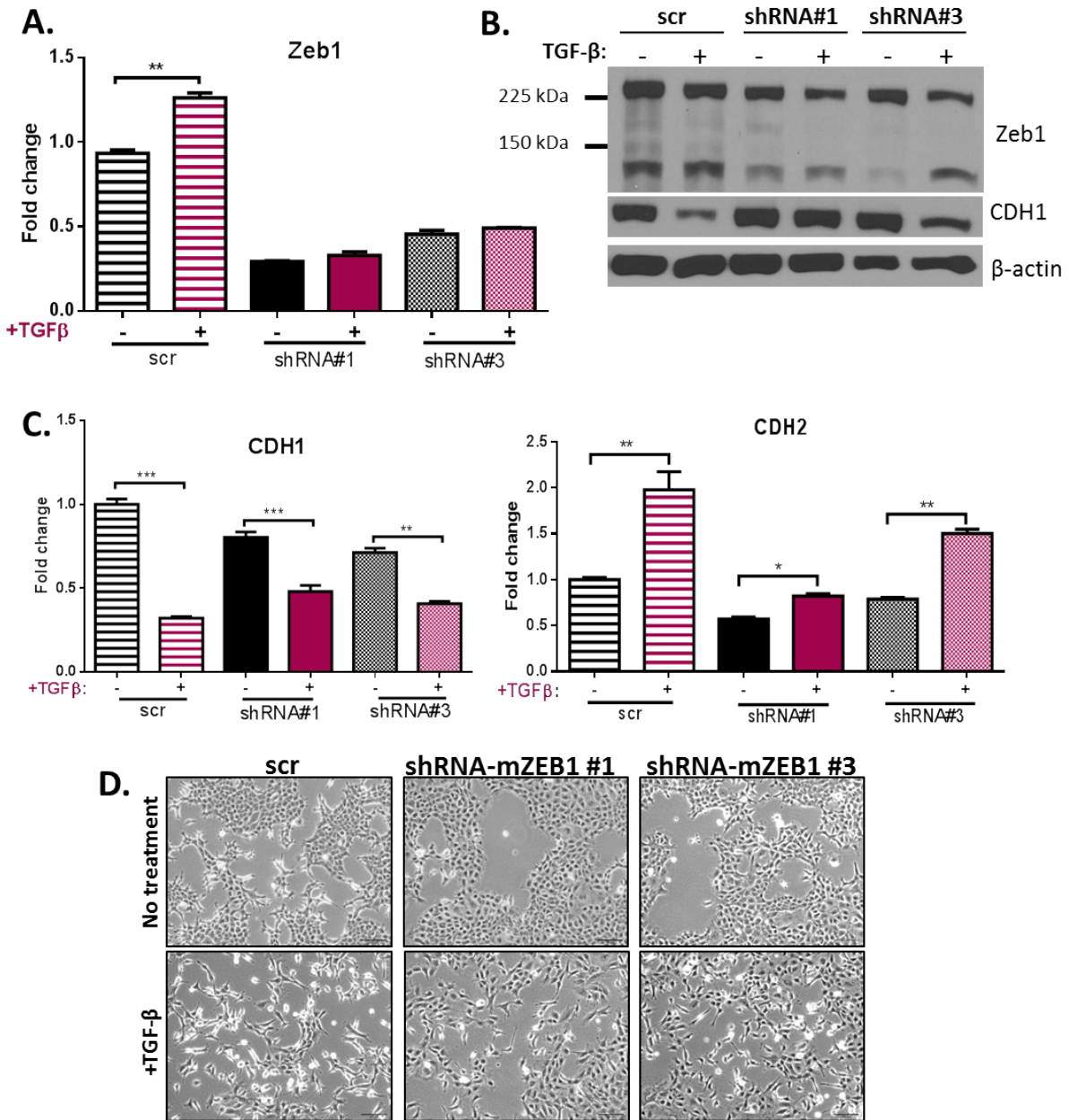


Fig.7 Knock down of Zeb1 in invasive cells does not effect response to TGF-β. (A) Syber Green-based qRT-PCR confirms Zeb1 knockdown and response to TGF-β as compared to scramble. Samples were treated with 5 ng/ml TGF-β for 96h as indicated. (B) Western blot analysis of 344SQ Zeb1 knockdowns treated as described above. (C) qRT-PCR of EMT markers for 344SQ Zeb1 knockdowns in 2D assays upon TGF-β treatment. (D) Morphology of 344SQ Zeb1-shRNAs treated with 5 ng/ml TGF-β for 96h.

ZEB1 was reduced (Fig. 7B). This indicates that upon TGF- β mediated EMT, 225 kDa-ZEB1 has a higher turnover and may contribute to the ZEB1 associated phenotype observed during EMT.

In order to better define whether Zeb1 knockdowns were capable of responding to TGF- β , knockdowns were grown in 3D MG/Col I and treated with TGF- β (Fig 8A). Once spheres formed (day 7), samples were treated with 5 ng/ml TGF- β for an additional 4 days. Notably, neither the scr nor the KD spheres formed a proper lumen. Similar to the response found in 2D culture, in 3D cultures Zeb1 knockdowns were still responsive to TGF- β , as assessed by changes to EMT markers at the mRNA level (Fig. 8D). All cell lines were hyper-proliferative as typically observed with TGF- β . These results suggest that ZEB1 is a redundant factor in metastasis and may not be required for TGF- β induced EMT, however further investigation must be conducted to confirm this conclusion.

Immunoprecipitation of GFP-tagged ZEB1

Given evidence that the higher molecular weight ZEB1 contributes to TGF- β mediated EMT and literature attributing this molecular weight difference to PTMs we sought to confirm and define the PTMs responsible for ZEB1 function. Potential Zeb1 PTMs were assessed by use of the 393P cell line expressing inducible GFP-tagged ZEB1 (393P-GFP-Zeb1) or control GFP (393P-GFP). After dox induction for 24 h, the GFP-ZEB1 or GFP production were confirmed by fluorescent imaging. ZEB1 was found localized to the nucleus in contrast to the vector control which produced GFP throughout the cell. 393P-TG-Zeb1 cells displayed a scattered, mesenchymal-like phenotype in 2D culture after 24 h (Fig. 2A). Whole cell lysates were then harvested from 393P-GFP-Zeb1 and 393P-GFP prior to ZEB1 immunoprecipitation (IP) using an anti-GFP antibody. The resulting protein was then separated by gel electrophoresis. As

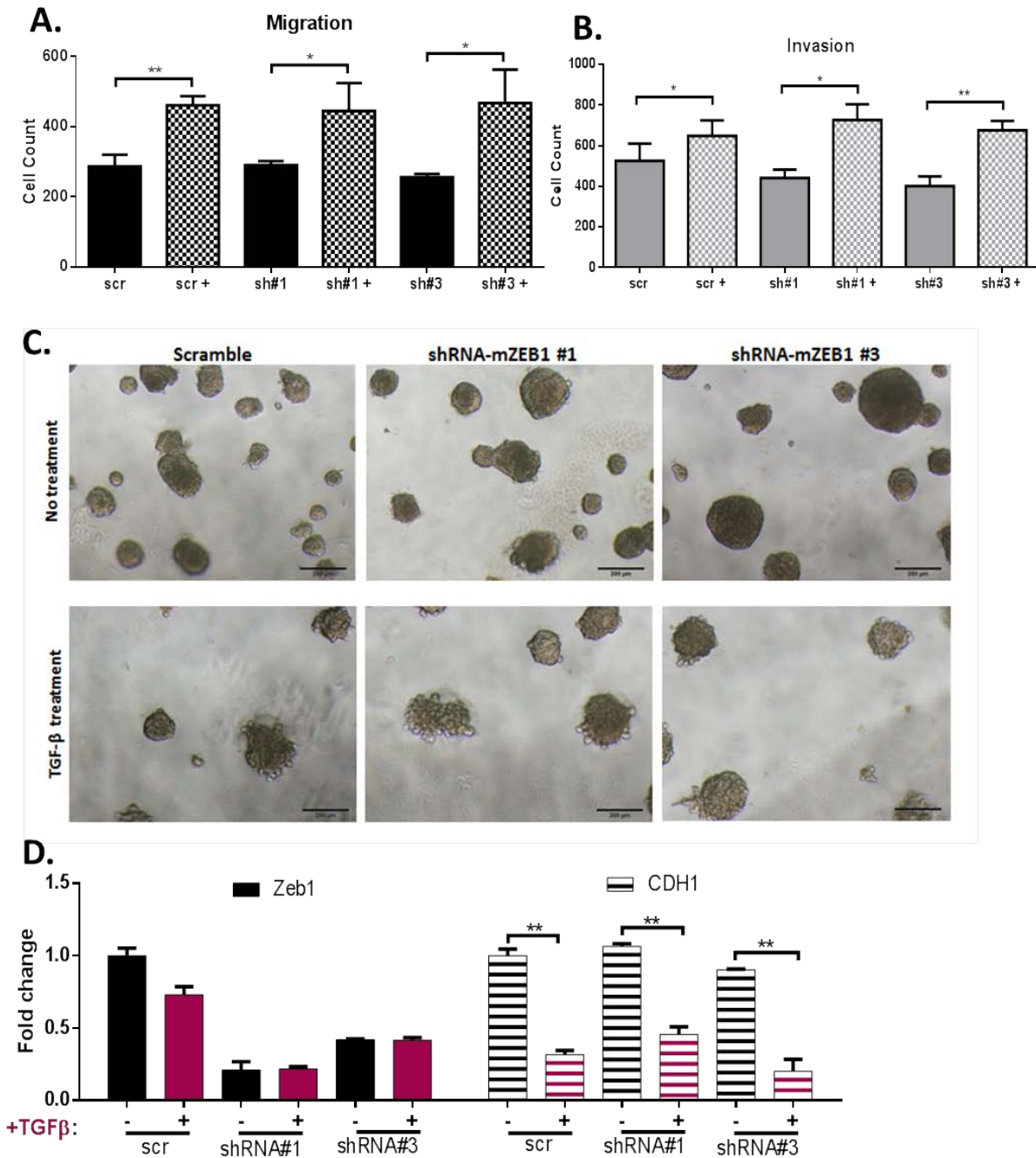


Fig. 8 3D-culture of Zeb1 knockdowns confirms Zeb1 is not required for TGF- β mediated EMT (A) 344SQ knockdown cells were grown in 3D on MG/Col I mix, with or without TGF- β on day 7 of culture. This was followed by RNA purification. (B) Syber green-based qRT-PCR was used to compare EMT mRNA expression upon TGF- β treatment. Samples are compared to scramble untreated.

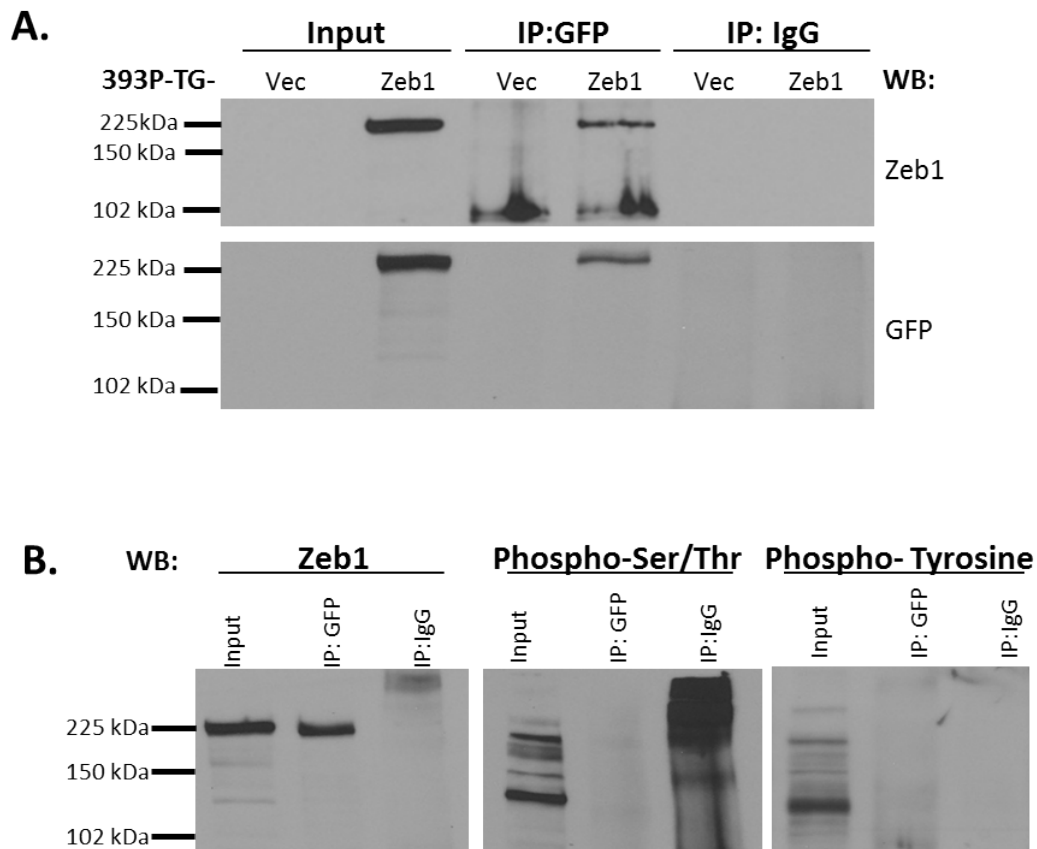


Fig. 9 Immunoprecipitation of the GFP-Zeb1 fusion protein. (A) 393P-GFP and Zeb1 cells were induced for 24 h for optimal GFP-ZEB1 expression. GFP antibody was used for IP as compared to IgG control. Western blot was then conducted. A signal was observed in the GFP-IP in the 393P-TG-Zeb1 (lane 4) corresponding with Zeb1 signal in input lysate (lane 2) while this was not observed in vector control GFP-IP (lane 3). (B) 393P-GFP-Zeb1 cells induced for 24 h were used for GFP-IP. Western blot was then conducted with primary antibody listed above each blot. No signal corresponding to GFP-ZEB1 fusion protein was detected by either phospho-ser/thr or phospho-tyr primary antibody (lane 2 of each blot).

expected, the GFP-ZEB1 fusion protein (250 kDa) appeared at approximately 25 kDa larger than the highest molecular weight form of ZEB1 (225 kDa) when probed by ZEB1 or GFP (Fig. 3B).

To determine specific ZEB1 PTMs, GFP-IP was performed with the 393P-GFP-Zeb1 whole cell lysate followed by immunoblotting with various anti-PTM antibodies. Since phosphorylation is one of the most common PTMs contributing to protein regulation, we initially immunoblotted for phospho-Serine/Threonine and phospho-Tyrosine. No signal was detected corresponding to the molecular weight of ZEB1 after IP for GFP (Fig. 9B). This result suggested that ZEB1 is not phosphorylated. Lambda phosphatase (lambda PP) incubation was then performed to confirm this result. Both murine (393P and 344SQ) and human (H441, H358, H1299, and H157) NSCLC cell lines were harvested in either PMP buffer and incubated with lambda PP or in RIPA buffer containing phosphatase inhibitors as a control. Western blot was then performed using the phospho-Ser/Thr antibody to determine whether the treatment was effective and indeed no phospho-Ser/Thr signal remained after treatment (lower panel of Fig. 10A & 10B). The same blots were then stripped and probed with the anti-ZEB1 antibody. The signal was reduced in the samples which were harvested in PMP buffer alone when compared to the RIPA buffer, however, the molecular weight of ZEB1 was not affected by the PMP buffer lysis in the cell lines 393P, 344SQ, H157 and H1155. In these samples incubation with phosphatase produced a significant ZEB1 molecular weight difference as compared to samples harvested in PMP buffer alone, suggesting that ZEB1 is in fact phosphorylated (upper panel of Fig. 10A & 10B). Interestingly, there was approximately 10 kDa difference in the ZEB1 molecular weight between samples lysed in PMP buffer alone (Fig. 10A, lane 2 and lane 5) compared to those incubated in lambda PP (Fig. 10A, lane 3 and lane 6) in the murine cell lines while there

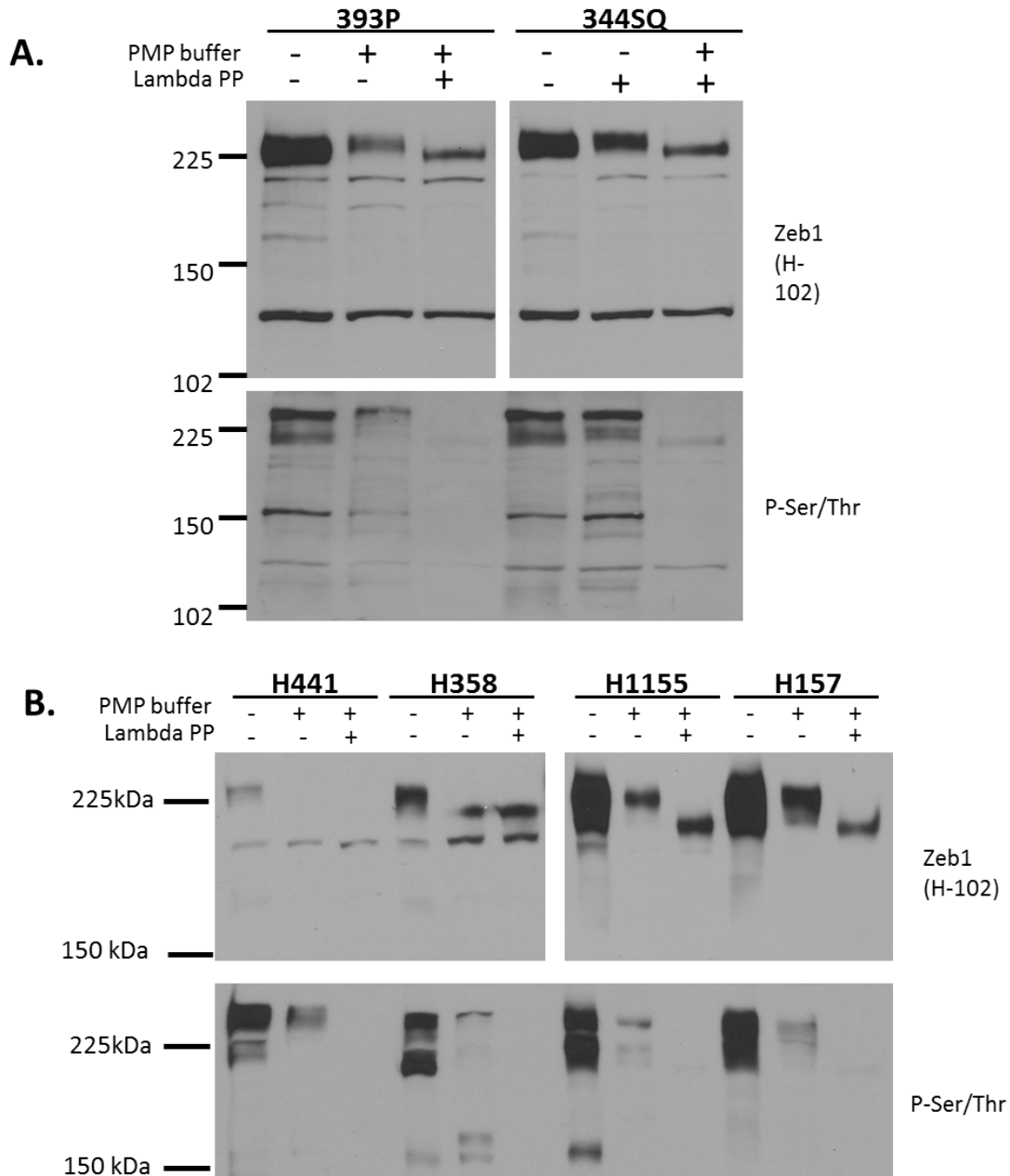


Fig. 10 Lambda phosphatase treatment of NSCLC cell lines confirms ZEB1 phosphorylation.

(A) Lysates of murine cell lines 393P and 344SQ were isolated in either RIPA or PMP buffer before samples were treated with lambda PP. Samples were then separated by gel electrophoresis. Phospho-Ser/Thr blot confirmed PP treatment (lane 3 and 6). In the upper Zeb1 blot a shift was observed in the 225 kDa-Zeb1. (B) Human non-small cell lung cancer cell lines were treated as in (A). A significant molecular weight shift was observed in the higher molecular weight ZEB1 from the H1155 and H157 cell lines. The H441 and H358 cell lines are regarded as non-invasive, epithelial cell lines and no shift was observed between the treated and untreated cells harvested in PMP buffer. In each panel the Phospho-Ser/Thr blots show the efficacy of phosphatase treatment.

was 20 kDa difference in the human NSCLC cell lines (Fig. 10B lanes 8 and lane 11 compared to lane 9 and lane 12). This may be due to differential phosphorylation in murine versus human ZEB1.

We next wanted to address if ZEB1 is acetylated as previously described [17]. In addition, we wanted to address whether the IP conditions or the antibodies were responsible for the inconsistent phosphorylation results. The cell line H157 which has high expression of ZEB1 was used to IP for endogenous ZEB1 followed by immunoblotting with an acetylated-lysine antibody (Fig. 11A). Notably, nothing was seen by western blot in the input (whole cell lysate) lane leading us to conclude that this antibody is not useful for analysis of ZEB1 acetylation. The inverse experiment was also conducted in which the anti-acetylated-lysine antibody was used to IP all acetylated proteins found in the whole cell lysate followed by immunoblot with ZEB1 antibody (Fig. 11B). No signal corresponding to ZEB1 was observed by either method suggesting that ZEB1 is not acetylated or that the lysis conditions are not suitable for ZEB1 IP.

Post-translational modification prolongs the half-life of ZEB1 protein

PTMs frequently play a role in the function of cellular proteins by affecting protein stability. To assess the role of PTMs on ZEB1 stability, a cycloheximide chase experiment was conducted. Cycloheximide (CHX) inhibits protein biosynthesis by arresting DNA translation through binding of the 60S ribosomal unit, allowing the decay rate of a protein of interest to ZEB1- to be observed over time. A time course was conducted by treatment of the wild-type cell lines 393P and 344SQ with 100 µg/ml CHX for up to 24 h. Immunoblot of the time course

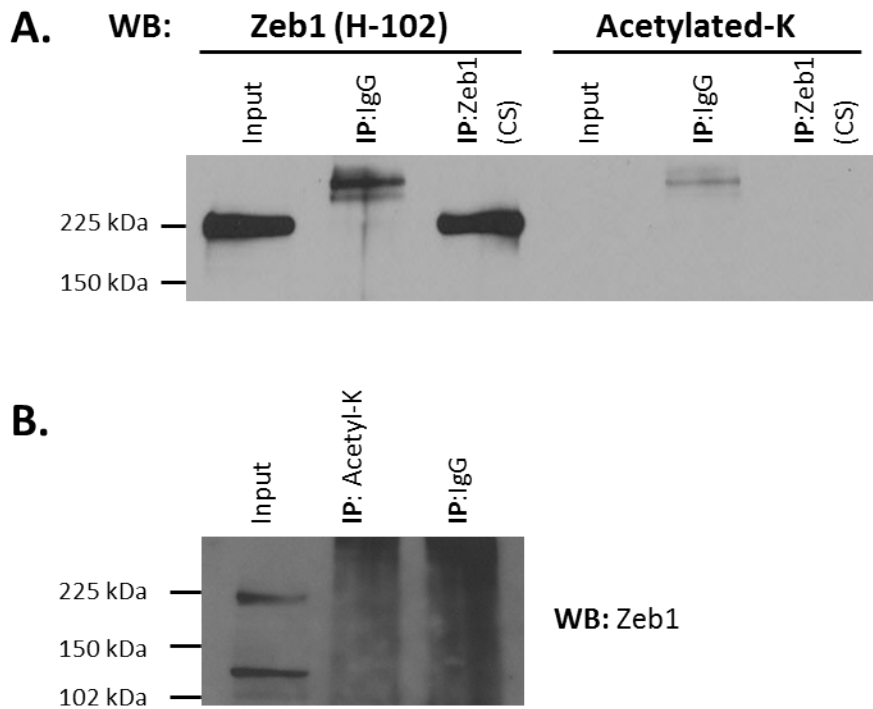


Fig. 11 Immunoprecipitation of the endogenous Zeb1. (A) H157 WT cells lysates were incubated with anti-Zeb1 antibody. IgG was used as internal control (lane 2 and 5). Western blot was then conducted. A signal was observed in the Zeb1 IP lane as compared to Input control confirming Zeb1 pull down. No signal was observed in Acetylated-lysine input control. (B) Acetylated-lysine used to IP (lane 2) all acetylated proteins found in the whole cell lysate followed by immunoblot with ZEB1 antibody.

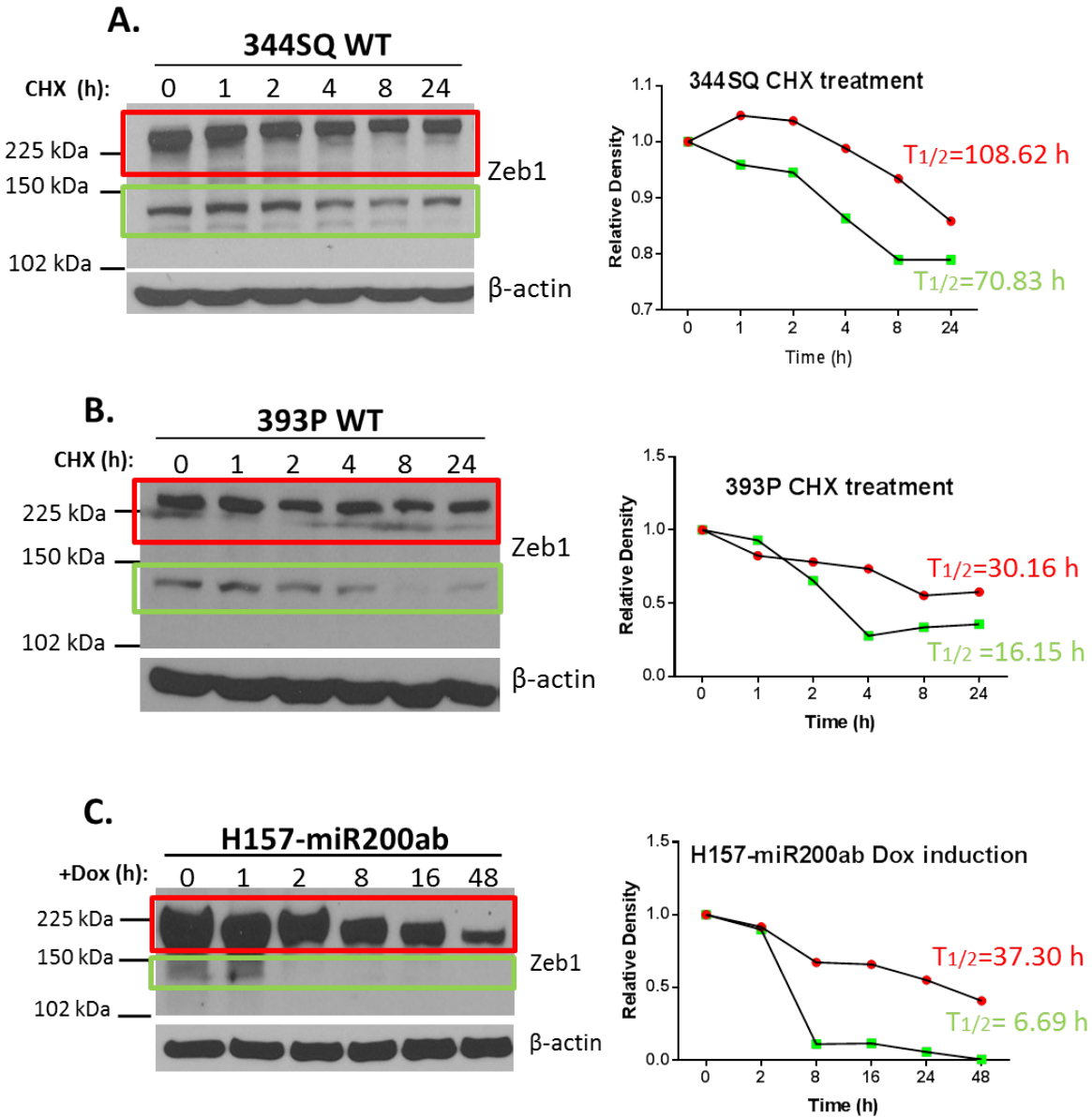


Fig. 12 Translational inhibition demonstrate differential effect between ZEB1 species. Red line: 225 kDa-ZEB1, green line: 125 kDa-ZEB1 (A) 344SQ cells and 393P cells (B) were exposed to 100 μ g/ml CHX for up to 24 h. Time points were collected as indicated. Quantification of results from panels are represented on the right of the corresponding figure. Half-life was calculated by $T_{1/2} = (\text{elapsed time} \times \log 2) / \log (\text{beginning amount} / \text{ending amount})$. (C) Time course of H157-miR200ab induced with dox for up to 48 h. $T_{1/2}$ was calculated as described.

experiment reflected a differential decay rate between the two observed molecular weights of ZEB1 in both cell lines (Fig 12A & 12B). Densitometry was performed using ImageJ software to quantify the half-life of both observed ZEB1 molecular weights. The half-life of the 225 kDa-ZEB1 was 30.16 h while the 125 kDa-ZEB1 was 16.15 h (Fig 12B) in 393P cells and in 344SQ cells the half-life was 108.62 h for 225-kDa ZEB1 and 70.83 h for 125 kDa-ZEB1 (Fig. 12A).

A similar experiment was conducted with the human NSCLC cell line H157 expressing both miR200a and miR200b upon dox induction (H157- miR200ab) [23]. The miR200 family is involved in a negative feedback loop with Zeb1 and is down-regulated in invasive cells. Dox induction of the H157 cells was conducted in a similar manner to the CHX time course experiment for 48 hours. Immunoblot revealed that again upon translational repression the expression of the lowest molecular weight ZEB1 was affected more than the higher molecular weight ZEB1 (Fig. 12C). Densitometry was conducted using ImageJ software to quantify the half-life of both observed ZEB1 molecular weights. After 48 h of miR200ab induction there was approximately 99% reduction of the lowest molecular weight ZEB1 while the highest molecular weight was not as prominently affected (reduced 59.02%). This data indicates that PTMs increase ZEB1 protein stability and prolong protein half-life.

BioID method can define the ZEB1 protein interactome

After complications with the IP procedure and inability to identify specific regulators of ZEB1 we decided to use the BioID method to determine protein interactions that may be responsible for ZEB1 modification. BioID allows for biotinylation of proteins that interact with a protein of interest fused to a mutated biotin ligase, BirA* [21]. These proximal proteins may

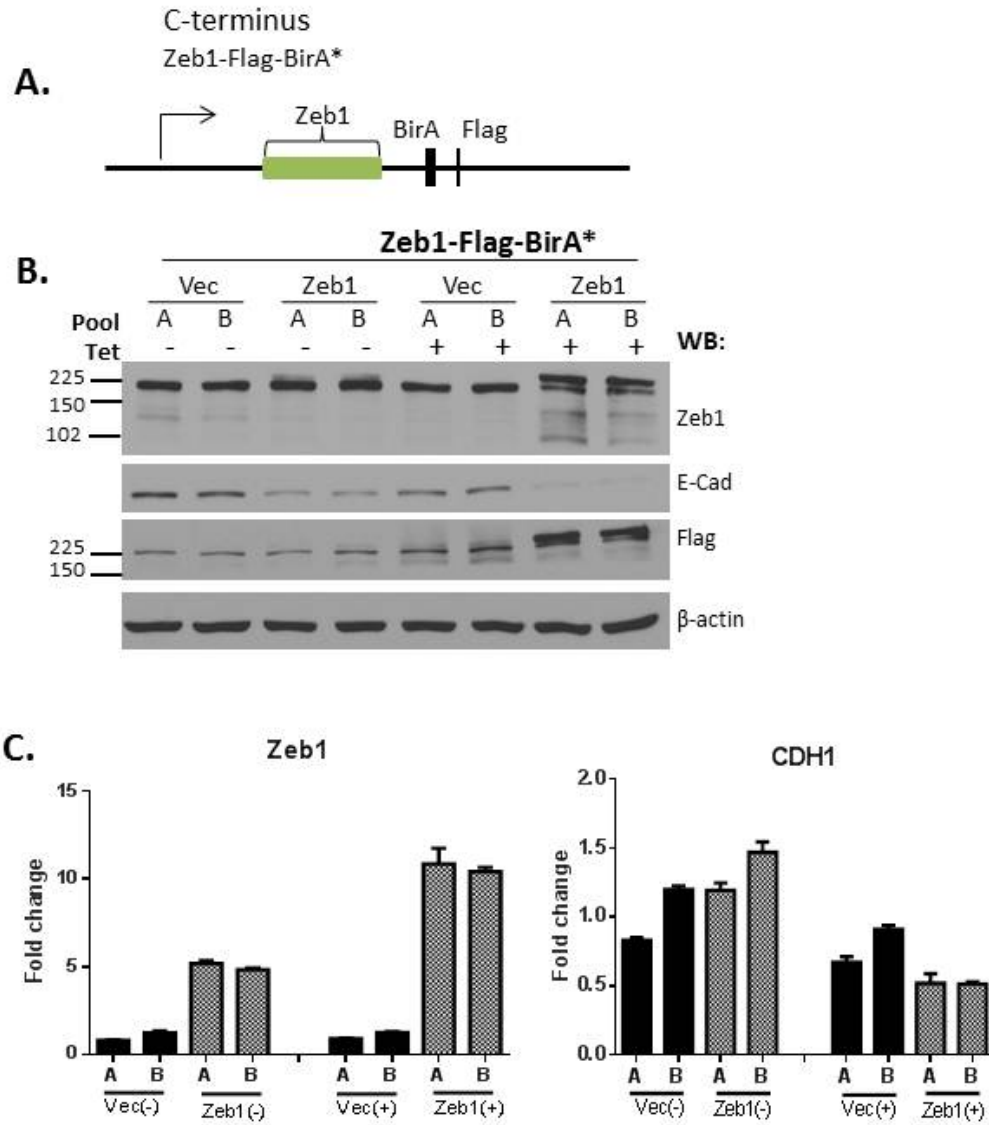


Fig. 13. C-terminus tagged Zeb1-Flag-BirA* is biologically active. (A) Diagram depicts the vector map of Zeb1-Flag-BirA*. (B) Western blot analysis verifying Zeb1 up-regulation upon tet induction as well as effects on the target gene E-Cadherin. (C) qRT-PCR of the indicated cell lines under tet induction confirms Zeb1 expression and biological activity.

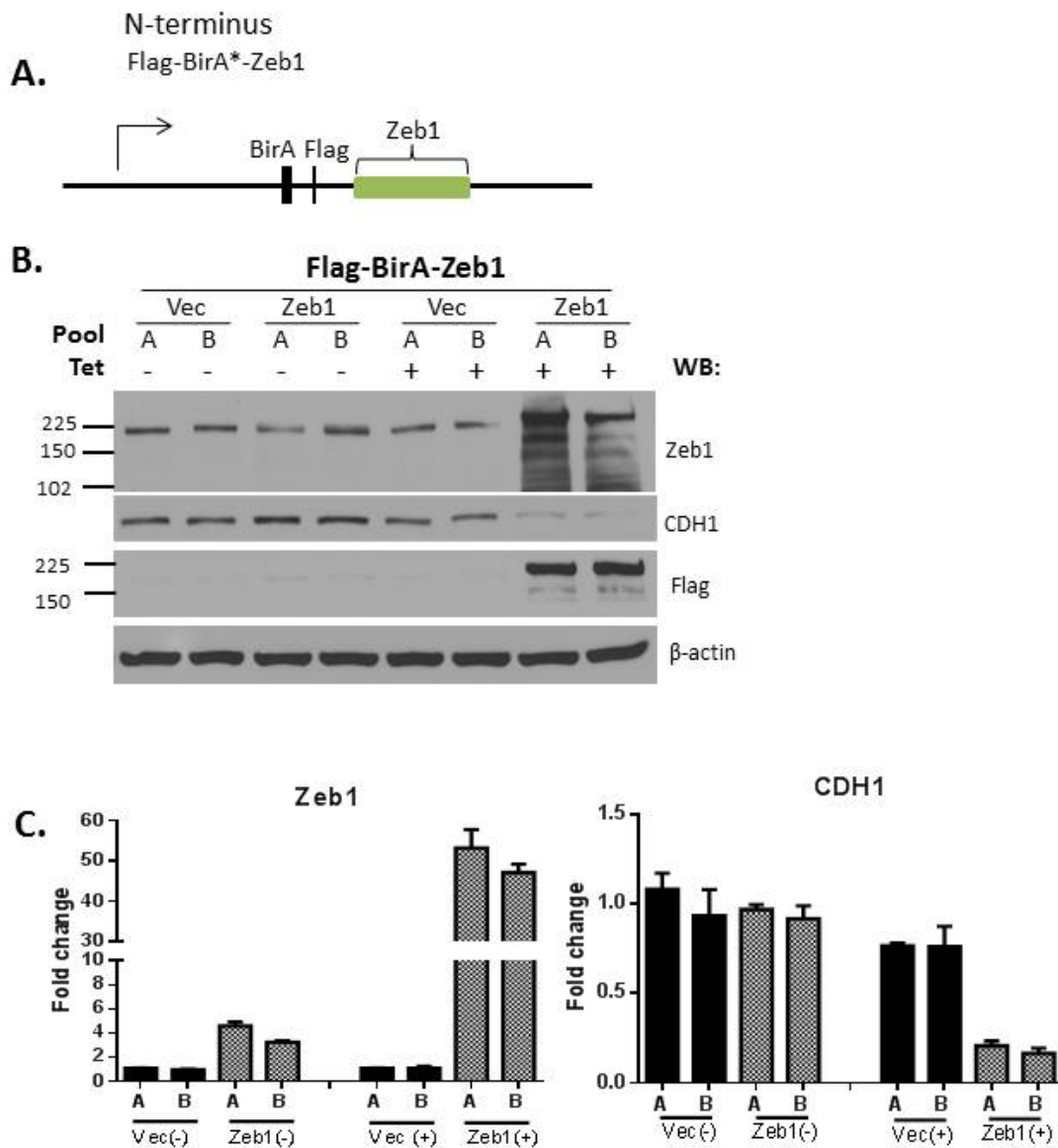


Figure 14. N-terminus tagged Zeb1-Flag-BirA* is biologically active. (A) Diagram depicts the vector map of Flag-BirA*-Zeb1. (B) Western blot analysis verifying Zeb1 upregulation upon tet induction as well as effects on the target gene E-Cadherin. (C) qRT-PCR of the indicated cell lines under tet induction confirms Zeb1 expression, biological activity, and significantly higher fold change than Zeb1-Flag-BirA*.

then be affinity captured and identified by mass spectrometry. Rather than using an affinity purification-based approach to identify proteins in a stable complex, the generation of the BirA*-ZEB1 fusion protein allows for identification of proteins which may act transiently or be involved in less stable interactions with ZEB1.

The human *Zeb1* cDNA was cloned into the previously described pcDNA5-FlagBirA-FRT/TO vector with the Flag-BirA* tag located at the N- or C- terminus (see Fig. 13A & 14A). The Flag-BirA* vector and *Zeb1* coding sequences were transfected into 293 T-Rex cells and cell pools with inducible tetracycline (tet) protein expression were selected. Both versions of the Flag-BirA*-Zeb1 fusion protein retained their biological activity as judged by repression of the target gene E-Cadherin by Western analysis (fig. 13B & 14B) and by qRT-PCR (Fig. 13C & 14C). The Flag-BirA* proteins alone were considered to be biologically inactive in all of these assays.

ZEB1 interactors will be identified from HEK/293 Flp-In cells grown under tet induction for 24h, along with the proteasomal inhibitor MG-132. As of now we are awaiting the results from the mass spectrometry analysis to differentiate between stable (Fig. 15A) and transient interactions (Fig. 15B).

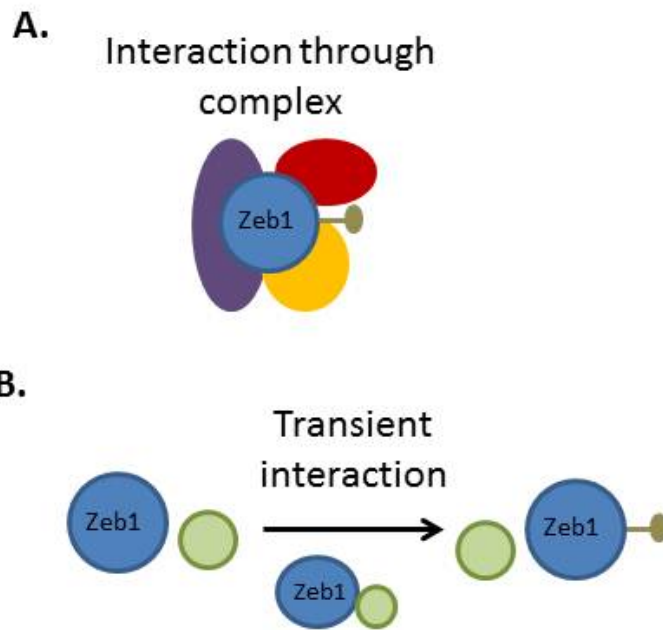


Figure 15. Schematic depicting potential interactions captured by BioID system. (A) BioID allows for biotinylation and capture of proteins which interact with Zeb1 in a stable complex or through (B) transient interactions.

Chapter 4:

Discussion

Discussion

Metastasis is a multi-step process in which cellular changes facilitate the loss of cell-cell contact enabling the primary tumor cells to invade distant sites. EMT is a proposed model for the initiation of tumor metastasis. During EMT epithelial cells gain a mesenchymal-like phenotype, promoting cell migration and subsequent invasion. The transcription factor ZEB1 is a well-established facilitator of EMT through the regulation of genes such as E-Cadherin, which are responsible for specialized cell contact. Zeb1 has been shown to be up-regulated in metastatic lung cancer [24] and recent research has shown Zeb1 depletion can overcome radiation and chemotherapy resistance [15, 25]; thus finding ZEB1-targeting agents has the potential to eradicate highly invasive tumors. Despite research on the role of Zeb1 as a regulator of EMT [13], a complete knowledge of ZEB1 interactors and their contribution to EMT have yet to be defined. Regulation of ZEB1 expression through PTMs has been established by several groups, however the role of PTMs in regulating ZEB1 function during EMT have not been fully elucidated. Our study sought to uncover novel interactions which may facilitate PTM of ZEB1 and to better understand the role of these PTMs on ZEB1 function in NSCLC.

In human bile duct carcinoma ZEB1 was shown to be lysine-acetylated by the cofactors P300 and PCAF causing ZEB1 functional inhibition [17]. Our study was not able to duplicate these experiments in NSCLC cell lines. Instead, our findings indicate that ZEB1 is most likely heavily phosphorylated as determined by the lambda PP experiment (Fig. 10A & 10B). Although no signal was found for a phosphorylated protein in the GFP-Zeb1 IP experiment (Fig. 9B), this

conflicting result may be due to the harsh lysis and washing conditions inhibiting Western blot antibody signal. Further experimentation must be conducted to validate these findings.

Considering that phosphorylation status is known to be important for protein-protein interactions (PPI) and protein stability, turnover experiments were performed using both murine and human cells. Previously, Zhang et al. researched the turnover of ZEB1 in radiation resistant subpopulations of breast cancer cells [15]. The investigators concluded that ZEB1 half-life was increased by phosphorylation, however the actual calculated half-life estimate was not provided. We disclosed the half-life of the endogenous ZEB1 in both murine cell lines through the use of protein synthesis inhibitors and for the human H157 cell line by use of an inducible miR-200ab model. We were also able to distinguish a differential effect between the two species of ZEB1 (Fig. 12A and 12B). The mechanisms underlying these intriguing findings remain unclear; nonetheless, the data suggests the importance of PTMs to ZEB1 protein stability.

While this study was in progress, Zhang et. al. reported that ZEB1 is a substrate of the kinase ATM in a radiation resistant breast cancer cell line and to isolated ZEB1-interacting proteins by Tandem affinity purification-mass spectrometry (TAP-MS analysis) [15]. In contrast to our study, this research focused on proteins with stable interactions with ZEB1, which could be identified through affinity purification. This methodology would not be expected to uncover transient protein interactions. The BioID system recently was shown to overcome this obstacle in identifying PPIs and to present a comprehensive, high confidence interactome comparable to *in vivo* biological interactions [26]. In this study, two constructs were created, with the BirA* ligase fused to the C- or N- terminus (Fig. 13A & 14A). One of the two inducible BioID cell lines exhibited high expression in response to Dox induction (N-terminus tag; Fig. 14C), which will

allow us to compare between biological scenarios in which ZEB1 is expressed at low basal levels (such as in non-metastatic primary tumors) or high basal levels (metastatic tumors). Our next approach in this project will be to distinguish stable and transient interactions and to confirm the PPI in our murine model systems and potentially in human NSCLC patient samples.

Although the overexpression of ZEB1 in stable lines of 393P cells promotes cell invasion together with the loss of adherens junctions [22], inducible expression of ZEB1 was not sufficient to induce invasion in established 344SQ epithelial structures as determined by 3D assays (Fig. 5D). This suggested that Zeb1 is required for the invasive phenotype, as previously described; however Zeb1 expression is not sufficient to disassociate the pre-established epithelial state typically observed in early stage disease. In contrast, the use of TGF- β in the 344SQ-shRNA-Zeb1 cells was still able to facilitate an EMT, providing evidence that ZEB1 may not be required for the initiation of metastasis but instead may be responsible for the invasive phenotype seen in metastatic tumors. Arguably, the nearly 40% remaining mRNA ZEB1 expression may have contributed to the capacity of the KD cells to initiate EMT. Further in vivo experimentation using the 393P-GFP-Zeb1 cell line must be conducted to validate this conclusion.

Interestingly, there was again a discrepancy noted between the two species of ZEB1 in the 344SQ-shRNA-Zeb1 cell lines. The prominent effect of the Zeb1-shRNA on Zeb1 mRNA in both KD cell lines did not translate to the overall protein expression. This discrepancy promotes the hypothesis that PTMs modulate the protein half-life as the 125 kDa-Zeb1 was affected by KD, while 225 kDa-Zeb1 was not. Upon TGF- β treatment the 225 kDa-ZEB1 was reduced by treatment while the lower molecular weight was increased. This indicates that during TGF- β

mediated EMT the 225 kDa-ZEB1 has a higher turnover and also that PTMs are required for ZEB1 function in facilitating the invasive phenotype.

In conclusion, we confirm that ZEB1 has multiple PTMS, one of which is phosphorylation. We demonstrate that these PTMs contribute to ZEB1 protein stability and function. We also disclose that although ZEB1 expression promotes the invasive phenotype seen in metastatic tumor, ZEB1 may not be the primary cause of loss of epithelial polarity, one of the earliest signs of malignancy. Additional research must be performed to confirm this observation. Furthermore, this data together with those implicating ZEB1 in therapeutic resistance underscore the importance of defining ZEB1 interactors and highlights the suitability of these interactors as therapeutic targets.

Bibliography

1. Siegel, R., D. Naishadham, and A. Jemal, *Cancer statistics, 2013*. CA Cancer J Clin, 2013. **63**(1): p. 11-30.
2. Larsen, J.E. and J.D. Minna, *Molecular biology of lung cancer: clinical implications*. Clin Chest Med, 2011. **32**(4): p. 703-40.
3. Zheng, S., A.K. El-Naggar, E.S. Kim, J.M. Kurie, and G. Lozano, *A genetic mouse model for metastatic lung cancer with gender differences in survival*. Oncogene, 2007. **26**(48): p. 6896-904.
4. Gibbons, D.L., W. Lin, C.J. Creighton, Z.H. Rizvi, P.A. Gregory, G.J. Goodall, N. Thilaganathan, L. Du, Y. Zhang, A. Pertsemlidis, and J.M. Kurie, *Contextual extracellular cues promote tumor cell EMT and metastasis by regulating miR-200 family expression*. Genes Dev, 2009. **23**(18): p. 2140-51.
5. Thiery, J.P., H. Acloque, R.Y. Huang, and M.A. Nieto, *Epithelial-mesenchymal transitions in development and disease*. Cell, 2009. **139**(5): p. 871-90.
6. Kalluri, R. and R.A. Weinberg, *The basics of epithelial-mesenchymal transition*. J Clin Invest, 2009. **119**(6): p. 1420-8.
7. Zhang, P., Y. Sun, and L. Ma, *ZEB1: At the crossroads of epithelial-mesenchymal transition, metastasis and therapy resistance*. Cell Cycle, 2015. **14**(4): p. 481-7.
8. Hashiguchi, M., S. Ueno, M. Sakoda, S. Lino, K. Hiwatashi, K. Minami, K. Ando, Y. Mataka, K. Maemura, H. Shinchi, S. Ishigami, and S. Natsugoe, *Clinical implication of ZEB-1 and E-Cadherin expression in hepatocellular carcinoma.pdf*. BMC Cancer, 2013. **13**(572).
9. Siebzehnrubl, F.A., D.J. Silver, B. Tugertimur, L.P. Deleyrolle, D. Siebzehnrubl, M.R. Sarkisian, K.G. Devers, A.T. Yachnis, M.D. Kupper, D. Neal, N.H. Nabilsj, M.P. Kladdé, O. Suslov, S. Brabletz, T. Brabletz, B.A. Reynolds, and D.A. Steindler, *The ZEB1 pathway links*

- glioblastoma initiation, invasion and chemoresistance*. EMBO Mol Med, 2013. **5**(8): p. 1196-212.
10. Matsubara, D., Y. Kishaba, T. Yoshimoto, Y. Sakuma, T. Sakatani, T. Tamura, S. Endo, Y. Sugiyama, Y. Murakami, and T. Niki, *Immunohistochemical analysis of the expression of E-cadherin and ZEB1 in non-small cell lung cancer*. Pathol Int, 2014. **64**(11): p. 560-8.
 11. Aigner, K., B. Dampier, L. Descovich, M. Mikula, A. Sultan, M. Schreiber, W. Mikulits, T. Brabletz, D. Strand, P. Obrist, W. Sommergruber, N. Schweifer, A. Wernitznig, H. Beug, R. Foisner, and A. Eger, *The transcription factor ZEB1 (deltaEF1) promotes tumour cell dedifferentiation by repressing master regulators of epithelial polarity*. Oncogene, 2007. **26**(49): p. 6979-88.
 12. Eger, A., K. Aigner, S. Sonderegger, B. Dampier, S. Oehler, M. Schreiber, G. Berx, A. Cano, H. Beug, and R. Foisner, *DeltaEF1 is a transcriptional repressor of E-cadherin and regulates epithelial plasticity in breast cancer cells*. Oncogene, 2005. **24**(14): p. 2375-85.
 13. Gregory, P.A., A.G. Bert, E.L. Paterson, S.C. Barry, A. Tsykin, G. Farshid, M.A. Vadas, Y. Khew-Goodall, and G.J. Goodall, *The miR-200 family and miR-205 regulate epithelial to mesenchymal transition by targeting ZEB1 and SIP1*. Nat Cell Biol, 2008. **10**(5): p. 593-601.
 14. Korpala, M., E.S. Lee, G. Hu, and Y. Kang, *The miR-200 family inhibits epithelial-mesenchymal transition and cancer cell migration by direct targeting of E-cadherin transcriptional repressors ZEB1 and ZEB2*. J Biol Chem, 2008. **283**(22): p. 14910-4.
 15. Zhang, P., Y. Wei, L. Wang, B.G. Debeb, Y. Yuan, J. Zhang, J. Yuan, M. Wang, D. Chen, Y. Sun, W.A. Woodward, Y. Liu, D.C. Dean, H. Liang, Y. Hu, K.K. Ang, M.C. Hung, J. Chen, and L. Ma, *ATM-mediated stabilization of ZEB1 promotes DNA damage response and radioresistance through CHK1*. Nat Cell Biol, 2014. **16**(9): p. 864-75.

16. Long, J., D. Zuo, and M. Park, *Pc2-mediated sumoylation of Smad-interacting protein 1 attenuates transcriptional repression of E-cadherin*. *J Biol Chem*, 2005. **280**(42): p. 35477-89.
17. Mizuguchi, Y., S. Specht, J.G. Lunz, 3rd, K. Isse, N. Corbitt, T. Takizawa, and A.J. Demetris, *Cooperation of p300 and PCAF in the control of microRNA 200c/141 transcription and epithelial characteristics*. *PLoS One*, 2012. **7**(2): p. e32449.
18. Chung, D.W., R.F. Frausto, L.B. Ann, M.S. Jang, and A.J. Aldave, *Functional impact of ZEB1 mutations associated with posterior polymorphous and Fuchs' endothelial corneal dystrophies*. *Invest Ophthalmol Vis Sci*, 2014. **55**(10): p. 6159-66.
19. Kundu, S.T., L.A. Byers, D. Peng, J.D. Roybal, L. Diao, J. Wang, P. Tong, C.J. Creighton, and D. Gibbons, *Foxf2 induces EMT and metastasis in lung cancer*. *Oncogene*, 2015.
20. Brown, C.Y., T. Sadlon, T. Gargett, E. Melville, R. Zhang, Y. Drabsch, M. Ling, C.A. Stratthdee, T.J. Gonda, and S.C. Barry, *Robust, reversible gene knockdown using a single lentiviral short hairpin RNA vector*. *Hum Gene Ther*, 2010. **21**(8): p. 1005-17.
21. Roux, K.J., D.I. Kim, M. Raida, and B. Burke, *A promiscuous biotin ligase fusion protein identifies proximal and interacting proteins in mammalian cells*. *J Cell Biol*, 2012. **196**(6): p. 801-10.
22. Ahn, Y.H., D.L. Gibbons, D. Chakravarti, C.J. Creighton, Z.H. Rizvi, H.P. Adams, A. Pertsemlidis, P.A. Gregory, J.A. Wright, G.J. Goodall, E.R. Flores, and J.M. Kurie, *ZEB1 drives prometastatic actin cytoskeletal remodeling by downregulating miR-34a expression*. *J Clin Invest*, 2012. **122**(9): p. 3170-83.
23. Chen, L., D.L. Gibbons, S. Goswami, M.A. Cortez, Y.H. Ahn, L.A. Byers, X. Zhang, X. Yi, D. Dwyer, W. Lin, L. Diao, J. Wang, J.D. Roybal, M. Patel, C. Ungewiss, D. Peng, S. Antonia, M. Mediavilla-Varela, G. Robertson, S. Jones, M. Suraokar, J.W. Welsh, B. Erez, Wistuba, II, L. Chen, D. Peng, S. Wang, S.E. Ullrich, J.V. Heymach, J.M. Kurie, and F.X. Qin,

- Metastasis is regulated via microRNA-200/ZEB1 axis control of tumour cell PD-L1 expression and intratumoral immunosuppression.* Nat Commun, 2014. **5**: p. 5241.
24. Gibbons, D.L., W. Lin, C.J. Creighton, S. Zheng, D. Berel, Y. Yang, M.G. Raso, D.D. Liu, Wistuba, II, G. Lozano, and J.M. Kurie, *Expression signatures of metastatic capacity in a genetic mouse model of lung adenocarcinoma.* PLoS One, 2009. **4**(4): p. e5401.
25. Ren, J., Y. Chen, H. Song, L. Chen, and R. Wang, *Inhibition of ZEB1 reverses EMT and chemoresistance in docetaxel-resistant human lung adenocarcinoma cell line.* J Cell Biochem, 2013. **114**(6): p. 1395-403.
26. Dingar, D., M. Kalkat, P.K. Chan, T. Srikumar, S.D. Bailey, W.B. Tu, E. Coyaud, R. Ponzielli, M. Kolyar, I. Jurisica, A. Huang, M. Lupien, L.Z. Penn, and B. Raught, *BioID identifies novel c-MYC interacting partners in cultured cells and xenograft tumors.* J Proteomics, 2014.

Vita

Roxsan Manshouri was born in Houston, Texas on September 7, 1990, the daughter of Taghi Manshouri and Mary Jane Manshouri. She received the degree of Bachelor of Science with a major in Biology in May 2013. She entered the University of Texas Graduate School of Biomedical Science at Houston and joined Don L. Gibbons' lab in August of 2013.

Permanent address:

1885 El Paseo St. Apt 149
Houston, Texas 77054